Journal of
Mechanical
Science and
Technology

Journal of Mechanical Science and Technology 21 (2007) 1090~1099

Research on Entirely-integrated Spatial-bending Shape Memory Alloy Actuator

Kai Yang*, Chenglin Gu

College of Electrical and Electronic Engineering, Huazhong University of Science and Technology, Wuhan 430074, Hubei province, People's Republic of China

(Manuscript Received October 29, 2006; Revised March 29, 2007; Accepted March 30, 2007)

Abstract

A new structure of Entirely-integrated Spatial-bending Shape Memory Alloy Actuators (ESSMAA) is first presented. Three SMA wires, which are trained to remember "U" recovery shape, are embedded in liquid silicone rubber to be solidified upon room temperature, companied with displacement sensors and connective wires. The Spatial bending, which is accomplished through heating SMA wires by suitable current, can restore flexibly as soon as stopping heating. Thus, the compact, two-way, mechanical and electrical incorporation actuator is completed. Be provided with the merits such as high load-weight ratio, low energy dissipation and direct driving, the actuators can realize miniature configuration, simple drive and control, precise operation and flexible movement pose synthetically. On the basis of expounding the operation principle in detail, the curvature sensor, which is composed of six stain gauges, makes displacement control precise. After analyzing equilibrium of forces and moments, the numeric calculation equations are deduced. Subsequently, the approximate arithmetic making use of superpose principle is researched in contrast with numeric arithmetic. The manufacture of the prototype is discussed in details and the precise displacement control is implemented also. Finally, the experiments of the actuator proof fine qualities of the operation performances.

Keywords: Entirely-integrated; Spatial-bending; Shape memory alloy actuator; Displacement control

1. Introduction

The mechanical design of a dexterous robotic hand, which utilizes non-classical types of actuation and information obtained from the study of biological systems, is becoming the interesting research field in recent years(Roh and Park, 2004; Guan and Zhang, 2003). Several unique and fascinating multi-degree-of-freedom robotic hands have been developed over the past twenty years, primarily using traditional means of actuation relying on electric, hydraulic or pneumatic technology. Unfortunately, there is a drastic reduction in the power that these forms of actuation can deliver as they are scaled down in size and weight.

This restriction has opened up investigation of several novel actuator technologies such as those relying on piezoelectrics, polymer gels, strictive effects, electrostatics and SMA(Bauer et al., 2006; Hu et al., 2006). Of these technologies, SMA actuators have a clear advantage in the strength–weight ratio. With the high inherent strength of SMA comes the advantage of being able to implement direct drive devices. Further, with the increased interest in mechatronics, SMA actuators with their silent, smooth and lifelike motions are easily adapted to miniaturization in design(Han et al., 2005; Singh et al., 2003). In 1984, Honma demonstrated that it is possible to control the amount of actuation by electric heating, thus opening their use in robotic applications

*Corresponding author. Tel.: +86 27 8754 3428, Fax.: +86 27 8754 3428
E-mail address: kkyhust@163.com

cations (Yoshiyuki et al., 1984). A biomechanic SMA hand that imitates the human hand in shape has been proposed(Mihalcz et al., 1999). The mechanical design of a SMA direct driven five finger robotic hand has been described in a recent US Patent(Rush, 1997). A SMA actuated micro-joint of a dexterous micro-gripper has been proposed(Troisfontaine, 1997). A novel SMA spring based actuator for force-feedback hand masters has been proposed(Burdea, 1995).

Though there has been much research accomplished on SMAs, there are still some disadvantages in the SMA-actuated robot hands. Firstly, the separation between actuating elements and executing elements is common in most configurations, which resulted in a complex structure and hampered their use in miniature systems. Secondly, their cartoon motions made grasping and fine manipulation very difficult. Thirdly, the degrees of freedom are limited. To solve these problems, a new type of entirely-integrated Spatial-bending SMA actuator is presented. It is proposed that the novel design methodology and prototype fabrication discussed in this paper will aid in the advancement and the development of human-like muscle actuators for assistive robotic devices and practical robotic systems.

2. Structure and mechanism

The Spatial-bending shape memory alloy actuator is developed by embedding three SMA wires with same specification, w_1, w_2 and w_3 respectively, to the rod symmetrically, as shown in Fig. 1. The distance between wires and neutral center of the rod is denoted with d. After being annealed at a certain temperature, the wire can memorize "U" curve and recover to the remembered shape when its temperature is raised above A_f, the austenite phase transition finish temperature. On the contrary, when the temperature of wire drops to M_s, the temperature when martensite phase transition begins, the Young's modulus of the SMA wire decreases immediately, which makes the wire bend easily.

According to the addible principle of motions, any two of the wires are selected to be heated to result in the flexural movement in 120 degrees range. So, the rod's Spatial movement can be realized by heating any two of the wires. Once the heat process stops, the actuator will return to its default state, a beeline, upon the rod's elasticity. Therefore, the actuator possesses the ability of operating Spatially.

To control the actuator precisely, proper feedback signals should be selected to construct a close-loop control system. It's an important procedure to choose suitable feedback signal. The conventional choice is the resistance of SMA wire. The control system based on resistance feedback aimed to get rid of complex sensors to make the mechanism compact as possible. Unfortunately, the precision is depressed greatly since SMA wire's resistance is not strictly monotone function of the curvature of the actuator. Accordingly, we choose the curvature of the actuator as feedback signal based on strain gauges. The sensor consists of six strain gauges divided to three groups: G_1G_4, G_2G_5, G_3G_6. All the gauges are distributed around the rod's surface with each interval angle 60 degree, as shown in Fig. 1. To eliminate the imbalance caused by fluctuation of the strain gauge's temperature during operation, half circuit bridge is used to obtain the actuator's curvature. When the actuator is in straight shape, the default state, the circuit bridge has zero output. Once the actuator runs, the curvature and moving direction are determined well and truly by the signals from curvature sensor. In order to heat the active SMA wires to reach their phases transformation temperature, A_s, currents with proper PWM width are input through conducting wires, which can be integrated in the rod solidified in room temperature. Therefore, the actuator is so called entirely-integrated Spatial-bending shape memory alloy actuator (ESSMAA).

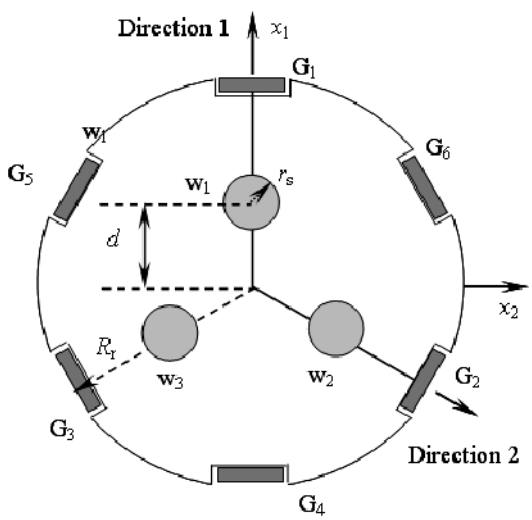

Fig. 1. Cross section of spatial bending SMA actuator.

3. Design and fabrication

3.1 Analytical model

Based on the results derived by Lagoudas and Tadjbakhsh(Brett and Dimitris, 1998), the deformation model of the rod with an off-axially embedded SMA wire is produced.

As shown in Fig. 2, the distributed forces, $\boldsymbol{f}$, acts on the rod from the SMA wire, with the offset of $\boldsymbol{d}$ from the actuation point to the neutral center of the rod. Firstly, analyzing the equilibrium of the rod, the vector form of the equations of equilibrium rod is expressed as follows:

$$\frac{\mathrm{d}\mathbf{F}}{\mathrm{d}S}+\mathbf{f}=0 \tag{1}$$

$$\frac{\mathrm{d}\mathbf{M}}{\mathrm{d}S}+\frac{\mathrm{d}\bar{\mathbf{x}}}{\mathrm{d}S}\times\mathbf{F}+\mathbf{m}=0 \tag{2}$$

where $\boldsymbol{F}$ represents the resultant force vector, $\boldsymbol{M}$ the resultant moment vector, $\boldsymbol{m}$ the moment caused by $\boldsymbol{f}$, S the arc length along the geometric center of the rod. The Eqs. (1) - (2) are solved in the body reference frame of the rod as:

$$\frac{\mathrm{d}F_{\mathrm{i}}}{\mathrm{d}S}+\varepsilon_{\mathrm{ijk}}k_{\mathrm{j}}F_{\mathrm{k}}+f_{\mathrm{i}}=0 \tag{3}$$

$$\frac{\mathrm{d}M_{\mathrm{i}}}{\mathrm{d}S}+\varepsilon_{\mathrm{ijk}}k_{\mathrm{j}}M_{\mathrm{k}}-(1+e)\varepsilon_{\mathrm{ij3}}F_{\mathrm{j}}+\varepsilon_{\mathrm{iak}}d_{\mathrm{a}}f_{\mathrm{k}}=0 \tag{4}$$

where i=1, 2, 3, j=1, 2, 3, k=1, 2, 3, a=1, 2. $\varepsilon_{\mathrm{ijk}}$ is 1 or -1 depending on the arrange of i, j and k.

Consider SMA wires, the vector form of the equation of equilibrium for the SMA wire is expressed as follows:

$$\frac{\mathrm{d}\boldsymbol{F}^{\mathrm{a}}}{\mathrm{d}z}+\boldsymbol{f}^{a}=0 \tag{5}$$

where z denotes the neutral axis of the SMA wire and $\boldsymbol{F}^{\mathrm{a}}$ represents the recovering force. From experimental results, the recovering force applied on the rod from the SMA wire with the memorized "U" curve can be regarded as the effect of equably distributed load. So, according to beam theory, the wire's recoverable curvature and recovering force have expressions as:

$$k'=\frac{qL^2}{8E^{\mathrm{a}}I^{\mathrm{a}}} \tag{6}$$

$$F^{\mathrm{a}}=qx \tag{7}$$

where E^{a}, I^{a} are elastic modulus and moment of inertia of the wire. q and L are load density and wire length respectively. The distance from calculation point to reference point is denoted by x. The internal recovering force $\boldsymbol{F}^{\mathbf{a}}$ is vertical to the wire's axis, i.e.

$$\boldsymbol{F}^{a}=F^{a}\boldsymbol{n} \tag{8}$$

The distributed force $\boldsymbol{f}^{\mathbf{a}}$, applied from the rod to the SMA wire and measured per unit length of the wire has in general the following resolution in the osculating plane:

$$\boldsymbol{f}^{a}=f_{\mathrm{t}}\boldsymbol{t}+f_{\mathrm{t}}\boldsymbol{n}$$

If the trihedral basis is used to resolve the vector form of the equations of equilibrium into components, the following set of two equations obtains (equilibrium in the osculating plane):

$$\frac{\mathrm{d}F^{\mathrm{a}}}{\mathrm{d}z}+f_{\mathrm{n}}=0 \tag{9}$$

$$-k_2F^{\mathrm{a}}+f_{\mathrm{t}}=0 \tag{10}$$

where k_2 denotes the wire's actual curvature, i.e. the actuator's curvature.

During the actuator's operation, if the wires w_1 and w_2 are heated simultaneously, Eqs. (3)-(4) are expressed as follows:

$$\frac{\mathrm{d}F_1}{\mathrm{d}S}+k_2F_3+f_1=0 \tag{11}$$

$$\frac{\mathrm{d}F_2}{\mathrm{d}S}-k_1F_3+f_2=0 \tag{12}$$

$$\frac{\mathrm{d}F_3}{\mathrm{d}S}+k_1F_2-k_2F_1+f_3=0 \tag{13}$$

$$\frac{\mathrm{d}M_1}{\mathrm{d}S}-(1+e)F_2+m_1=0 \tag{14}$$

$$\frac{\mathrm{d}M_2}{\mathrm{d}S}+(1+e)F_1+m_2=0 \tag{15}$$

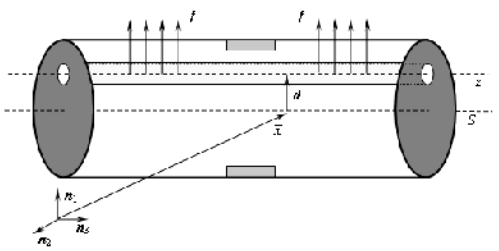

Fig. 2. Rod with an off-axis SMA wire.

where F_1 and F_2 are shear forces in the cross section of the rod, F_3 represents the axial component force, k_1, k_2 and k_3 are the two curvatures and twist of the rod, e the elongation of the rod, f_1' f_2' f_3' m_1 and m_2 are the component forces and moments applied on the rod from the wires.

The distributed force $\boldsymbol{f}$ applied on the rod from the SMA wire is connected through Newton's third law to the distributed force $\boldsymbol{f}^a$ applied from the rod to the SMA wire by

$$\boldsymbol{f} = -\boldsymbol{f}^a \tag{16}$$

Notice that to be able to find the components of $\boldsymbol{f}$ in terms of the components of $\boldsymbol{f}^a$, the distributed force $\boldsymbol{f}^a$ should be resolved in the body coordinate system as follows:

$$f_1 = f_1^1 + f_1^2 = \frac{\mathrm{d}F_1^a}{\mathrm{d}z} - \frac{1}{2}\left(\frac{\mathrm{d}F_2^a}{\mathrm{d}z}\right) \tag{17}$$

$$f_2 = f_2^1 + f_2^2 = \frac{\sqrt{3}}{2}\left(\frac{\mathrm{d}F_2^a}{\mathrm{d}z}\right) \tag{18}$$

$$f_3 = f_3^1 + f_3^2 = -k_2(F_1^a + F_2^a/2) - \sqrt{3}k_1F_2^a/2 \tag{19}$$

$$m_1 = d_2^2 f_3^2 = 3k_1F_2^a d/4 \tag{20}$$

$$m_2 = d_1^1 f_3^1 - d_1^2 f_3^2 = dk_2F_1^a - \sqrt{3}dk_1F_2^a/4 \tag{21}$$

where f_1^1, f_2^1 and f_3^1 are the components in directions x_1, x_2, and x_3 of the force applied on the rod from the wire w_1 respectively, d_1^1 denotes the component in direction x_1 of the offset of the wire w_1. Similarly, the superscript 2 indicates the relevant parameters of the wire w_2.

Combining Eqs. (11)-(21), the shape change of the actuator upon being actuated is calculated precisely by the numeric calculation using computer aided programming. However, the approximate arithmetic can be used to simplify the calculation. Actually, the elongation of the rod is small and can be ignored. Sine the internal force of the wire is vertical to its axis, F_3 is approximate equal to zero. Thus, the curvature of the rod with a single embedded SMA wire is produced as:

$$k_2 = \frac{k'}{\beta + d_1k'} \tag{22}$$

Where $\beta = EI/E^aI^a$, E and I are elastic modulus and moment of inertia of the rod. If the curvature of the rod upon only wire w_1 being actuated is expressed as k_{s1}, then

$$k_{s1} = \frac{k_1'}{\beta + dk_1'} \tag{23}$$

Where k_1' is the recoverable curvature of the SMA wire w_1. Virtually, there are three wires in the rod so that the parameter E should be modified as:

$$E = \frac{E^r(R^2 - 3r^2) + 3E^a r^2}{R^2}$$

Similarly, when the wire w_2 is heated alone, the curvature of the rod is expressed as

$$k_{s2} = \frac{k_2'}{\beta + dk_2'} \tag{24}$$

where k_2' is the recoverable curvature of the SMA wire w_2. The case when the wires w_1 and w_2 are heated simultaneously, the rod's final curvature obtains as:

$$k_{12} = \sqrt{(k_{s1})^2 + (k_{s2})^2 - k_{s1}k_{s2}} \tag{25}$$

The angle φ_{23} between the flexural plane and plane x_1x_3 is expressed as

$$\cos\theta_{23} = \frac{(k_{23})^2 + (k_{s3})^2 - (k_{s2})^2}{2 \quad k_{23} \quad k_{s3}} \tag{26}$$

3.2 Prototype fabrication

The rod is required to not only have good elasticity and strong stickiness to the SMA wires, but also vulcanize at room temperature without generating heat which might warm the SMA wires. If excess heat causes strain recovery before the SMA wires are bonded into the rod, no actuation strain will be available for actuating the rod. We searched for matrix materials for the ESSMAA and determined that a kind of single-component elastic moulding compound, RTV 515 (a room temperature vulcanizing silicone elastomer), provided the best properties. Tensile tests showed the elastic modulus of the elastomer to be 0.78 MPa. The rod length of 60 mm was selected, and the radius of the rod was determined by a parametric study of the rod deflection using the analytical model derived in section 3.1. The radius of the rod was designed to maximize the deflection of a rod with a single SMA wire with the restriction that the rod should return to

straight default state soon as possible. Finally, 5 mm of the radius was determined.

The next step in producing the prototype was preparation of SMA wires from saw, as annealed, Nitinol wire. This wire was received in a coil. In order to insure that the wire has a perfectly "U" memorized shape, it was decided to anneal the SMA wire while clamped in a "U" configuration through a certain heat treatment. The heat treatment for SMA wire to memorize the "U" curve can be realized by two means, namely, middle temperature process and low temperature process. Figure 3 shows the difference between these two means. It's explicit that the low temperature process has bigger recoverable curvature than that of the middle temperature process. So, the former manner was suitable.

While being annealed, the SMA wire should be carefully stained in "U" shape. To achieve this, a unique annealing jig was designed and fabricated from steel. This jig was designed to constrain the SMA in "U" shape and be heated in a furnace. A drawing of this jig appears below in Fig. 4.

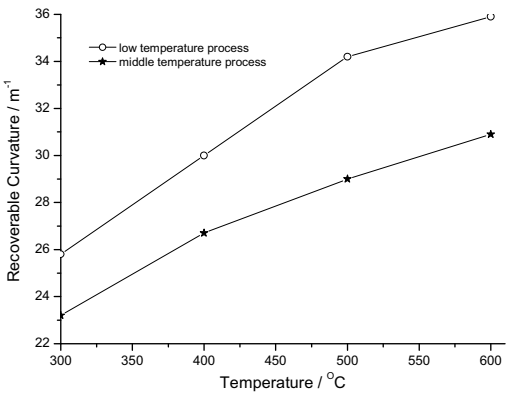

Fig. 3. Comparison between two heat treatments.

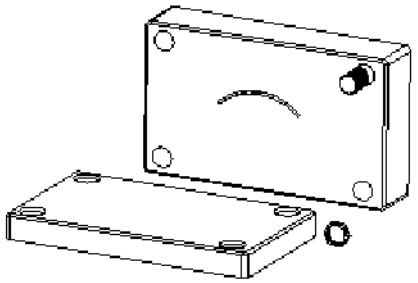

Fig. 4. Drawing of the mold for SMA preparation.

The following protocol was used to prepare the SMA wires:

(1) The SMA wire was cut into 60 mm lengths and located into the jig.

(2) Annealed at 400 degrees C for 1/2 hour in the local steel treater's furnace.

(3) Immerge in the water to cool down quickly.

(4) Strain SMA wires to straight shape.

When the rod's radius, R_r and length, L were determined, the wire's radius r_s has important influence on the characteristics of the actuator. Generally, the case that only the wire w_1 is heated is examined carefully. According to the analytical model, the simulated maximum curvature of the actuator, k_{max} is found to increase obviously through increasing r_s while the response speed slows down and actuator's remnants curvature, k_{left} is biggish after the wire's temperature falls below the room temperature. When the rod's radius and recoverable curvature of the wire are 5 mm and 57 m^{-1} respectively, the curve of $\alpha=k_{max}/k_{left}$ is shown in the Fig. 5. Obviously, it is interesting to see that the optimal radius is around 0.3 mm, where both the k_{max} and k_{left} have fine values. So, the wire 0.25 mm in radius was selected from the materials we can get.

In the ESSMAA, it is important to determine the offset d between SMA wires and the geometric center of the rod. Choose r_s=0.25 mm, R_r=5 mm and the wire's recoverable curvature k_r=57 m^{-1}, from Eq. (10), it is explicit that k_{max} is increasing with the decrease of d. On the other hand, too small d will result in heat disturbance among three wires. The temperature distribution in the ESSMAA when the wire w_1 is heated alone is considered, the temperature-current relationship of wire w_1, heated by electrical current

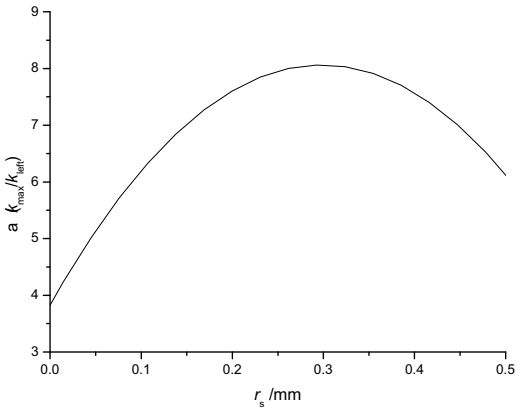

Fig. 5. k_{max}/k_{left} is a function of wire's radius.

Table 1. Specifications of the ESSMAA.

Names	Values
Rod's elastic modulus, E (MPa)	0.78
Rod's radius, R_r (mm)	5
Wire's austenitic elastic modulus (GPa)	83.3
Wire's martensite elastic modulus(GPa)	60.5
Length of the rod (mm)	60
Off-axial distance d (mm)	1.5
Wire's radius, r_s (mm)	0.25
Wire's recoverable curvature, k_r (m^{-1})	57

pulse, is derived using several simplifying assumptions. The most important assumption is that the heat capacity may be considered a constant lumped parameter. As the crystal structure of an SMA wire changes from martensite to austenite, or vice-versa, the specific heat capacity does not remain constant. Furthermore, heat capacity is physically a distributed parameter. However, the constant lumped parameter assumption is made to significantly simplify the analysis.

The temperature-current relationship is thus the direct application of conventional dynamic conduction and heat transfer models. The change in internal heat energy of the SMA wire must equal the energy delivered to the wire by the electrical current minus the energy transferred to the rod by conduction. Thus, in mathematical notation, the energy equation may be expressed as:

$$\rho_w c_w V_w \frac{dT_w}{dt} = d_r R i^2 - h_w A(T_w - T_0) \quad (27)$$

where ρ_w denotes density of the wire, c_w is specific heat of the wire, d_r the duty ratio of the current, V_s volume of the wire, T_w the wire's temperature, i represents the electrical current, R the wire's resistance, h_w the heat transfer coefficient and A is the surface area of the wire.

According to the temperature analysis model of the rod with embedded heat source(Bo et al., 1995), if heat current is 2 A, the temperature distributions in the rod at different time are described in Fig. 6. Obviously, after two seconds, the temperature distribution remains unchanged any longer since the system reach heat balance point. From those curves at different time, it is indicated that heat source has neglectable influence on the area where the distance from wire w_1 is more than 3 mm. Considering

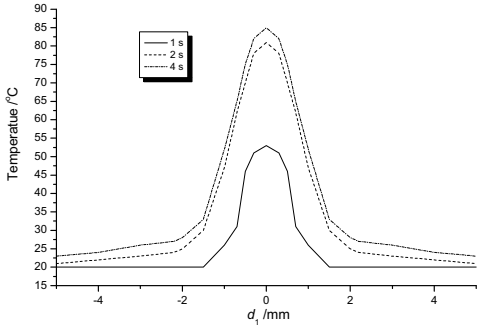

Fig. 6. Temperature distribution in rod upon w_1 being heated.

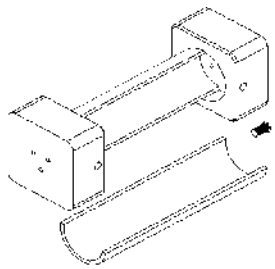

Fig. 7. Mold for actuator's fabrication.

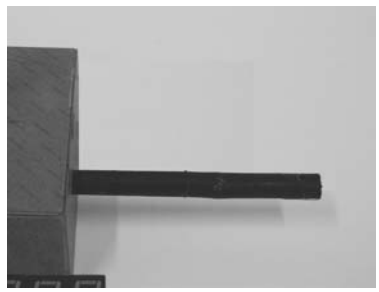

Fig. 8. Picture of the prototype.

restrictions of prototype's manufacture techniques synthetically, d=1.5 mm is appropriate for the ESSMAA.

After suitable material of the rod and SMA wires are selected and key parameters are determined, the next step is to prepare the actuator. First, a mold is constructed that could easily come apart for demolding, appearing in Fig. 7. The SMA wires are sandblasted, straightened, primed, and clamped into the mold and the silicone molding compound is degassed under vacuum to remove entrapped gas bubbles.

Finally, the material and geometrical parameters of designed ESSMAA prototype are summarized below and in Table 1. The picture of the prototype is shown in Fig. 8.

4. Deflection control

4.1 measurement of the curvature

The conventional feedback signal for control is the resistance of SMA wire. However, based on the experiments, the stability and veracity does not meet the real requirements very well. So, the external signal, i.e the curvature of the actuator is measured to carry out the control system. Presently, sensors for measuring curvature consist of fiber gratings and strain gauges. Compared with fiber gratings, strain gauges are cheaper and more feasible. Therefore, the curvature sensor consisting of six strain gauges is designed, shown in Fig. 1. When the actuator operates, two groups at most have positive outputs according to the set positive direction. If one group's output is much larger than the other, it's implied that the actuator bends along that direction and the curvature equals the output. When outputs of the two groups are comparable, the bending direction and the curvature are determined through addible theory by Eqs. (25) - (26).

The length change of the gauge has the following relation with its resistance change:

$$\frac{\Delta R}{R_s} = K\varepsilon_1 \tag{28}$$

where R_s is the standard resistance of the gauge, ΔR represents the resistance change, ε_1 denotes the strain and K is the sensitive coefficient depending on the material, configuration and geometry of the gauge. According to the dimension of the actuator and the experimental requirements, the length of the gauge should be long enough. Eventually, the semi-conductor gauge SY-120 with the length of 5~10 mm is used. Because of the difference of the elastic modulus of the gauge, rod and glue, companied with the effect of bond techniques, the stain of the gauge has the following relation with that of the actuator:

$$\varepsilon_1 = K_t \varepsilon_{\mathrm{ESMAA}} \tag{29}$$

where K_t represents the transfer coefficient. Combine Eqs. (28)-(29), the relation between the resistance change and the curvature of the actuator is expressed as:

$$\frac{\Delta R}{R} = KK_t \frac{R_r}{\rho} = KK_t R_r c = K_s c \tag{30}$$

where c denotes the actuator's curvature and K_s is defined as the measurement coefficient. In general, K_s is difficult to obtain from the theoretical manner. In our work, it is determined directly through experiments of measuring the resistance changes at several set points.

4.2 Control system

The transformations of SMA wire from austenite phase to martensite phase and vice-versa is observed by noting the volume fraction of martensite R_m, which varies between 0 (all austenite) and 1 (all martensite) and possesses the following relation with its temperature:

$$R_m(T) = \frac{R_{ma}}{[1 + e^{k_m (T - T_0)}]} + R_{mb} \tag{31}$$

where T represents the temperature of the SMA wrie, R_{ma} and R_{mb} are constants, k_m and T_{om} are constants depending on whether the wire being heated or cooled. Corresponding to transformation, R_m can be regarded as a quantitative index indicating the ratio of the transformation. Thus the relationship between recovering curvature k of the wire and the recoverable curvature k_{ms} of the wire is depicted as:

$$k = (1 - R_m) * k_{ms} \tag{32}$$

Combining Eqs. (31)-(32) and (27), the duty ratio of heating current obtain from the recovering curvature of the SMA wire.

In order to make ESSMAA realize the set motions, it is needed to plan the operations, i.e produce the series set points within the reachable space. Then, the actuator's curvatures at the set points obtain by the analytical model in Sec. 3.1, and which wire should be heated is also determined simultaneously. Furthermore, the duty ratios are determined and the plan manner is shown in Fig. 9.

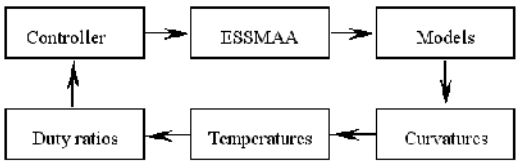

Fig. 9. Operation plan of ESSMAA.

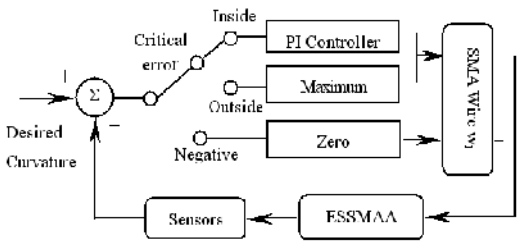

Fig. 10. Piecewise multimode controller for SMA wires.

A piecewise multimode controller, which is described in Fig. 10, has been explored for displacement control of the SMA wire. If the error is negative, then output zero. If the error is positive and large, then the maximum constant feedback is used. As the error approaches the critical point the control is switched to the PI controller. This results in a smoother motion of the actuator.

5. Results and discussion

When the deflections of the wires w_1 and w_2 reach the maximum simultaneously, i.e. the temperatures of two wires are above 83 °C, austenite phase transformation finish temperature, the components of flexural shape of the actuator in directions x_1 and x_2 are shown in Figs. (11)-(12). The solid curves indicate the approximate solution while the dashed represent numeric solution. From the comparison, the curvature error in direction x_1 is 3.5 % and 5.5 % in direction x_2. Therefore, it is concluded that the approximate solution is almost similar with the real situation.

When curvatures of the actuator in direction 1 are set as 5 m^{-1}, 6.25 m^{-1}, 7.14 m^{-1}, 8.3 m^{-1}, 10 m^{-1}, 12.5 m^{-1} and 14.3 m^{-1} respectively, the amplified voltages from the electrical bridge are fit linearly to determine the coefficient K_s 0.465 v·mm, as shown in Fig. 13.

The driving experiment was conducted. When the actuator operates by heating wires w_1 and w_2 simultaneously through a current supply with the magnitude of 2 A and the period of 15.4 ms, the relation between the actuator's curvature and the duty ratios is shown in Fig. 14. It's explicit that the curvature is near 0.8 at the beginning, and then increases quickly, finally reaches the maximum 28 m^{-1} as the duty ratio rises to 70 %.

Figure 15 shows step response result making use of Piecewise multimode controller. The target curvature is 10 m^{-1} and sampling time is 0.05 s. From the

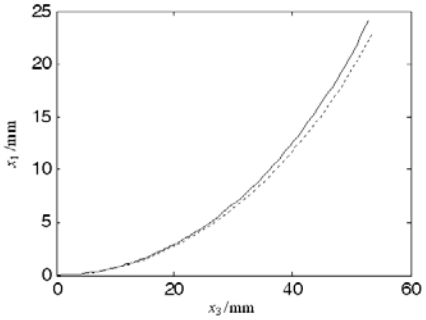

Fig. 11. Displacement along x_1 direction.

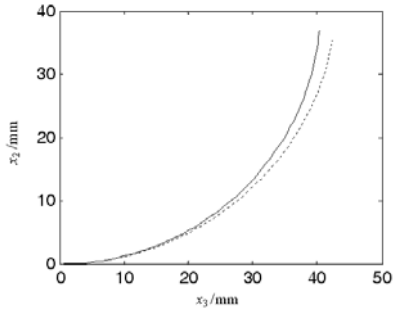

Fig. 12. Displacement along x_2 direction.

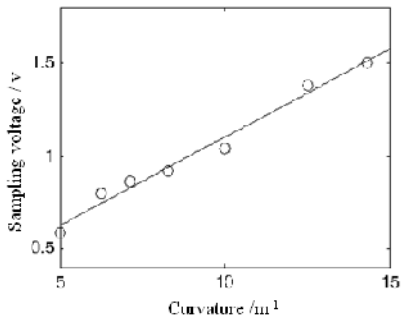

Fig. 13. Relationship between sampling voltage and curvature.

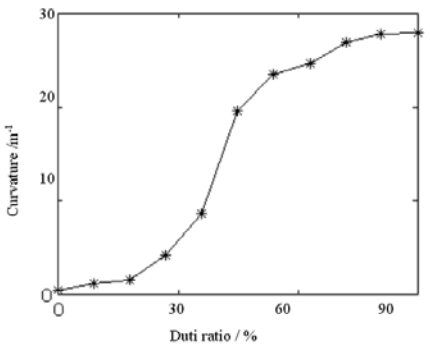

Fig. 14. Relationship between curvature and duty ratio of input pulse.

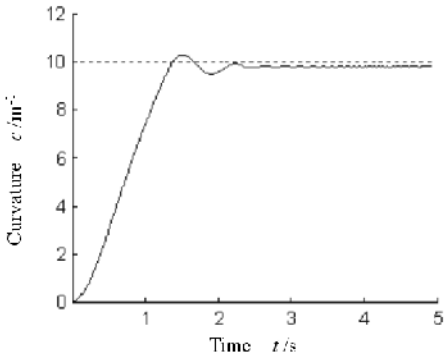

Fig. 15. Step response curve.

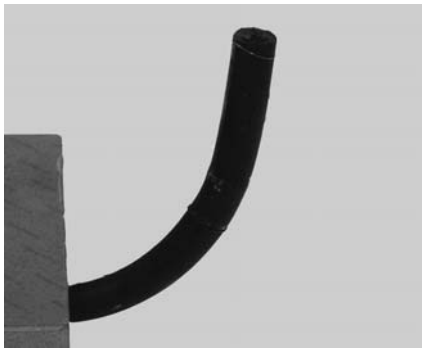

Fig. 16. Picture of the actuator upon being actuated.

observation, the rise time is 1.2 s, overshoot is 2%, steady error is 0.2 m^{-1} and the force output of the actuator's tip was measured to be 1.1 N. In Fig. 16, the actuator was shown to make a pliable motion at the velocity about 55 °/s up to the maximum angle between the tangents of two ends, 95 degrees relatively. The actuator is able to be used to manufacture the flexible robot hand and by controlling the heating of each SMA wire, the hand could accomplish Spatial movements flexibly.

6. Conclusion

A new structure of Entirely-integrated Spatial-bending Shape Memory Alloy Actuators (ESSMAA) is first presented. Three SMA wires, which are trained to remember "U" recovery shape, are embedded in liquid silicone rubber to be solidified upon room temperature, companied with displacement sensors and leading wires. The Spatial bending, which is accomplished through heating SMA wires by suitable current, can restore flexibly as soon as stopping heating. Thus, the compact, two-way, mechanical and electrical incorporation actuator is completed. Be provided with the merits such as high load-weight ratio, low energy dissipation and direct driving, the actuators can realize miniature configuration, simple drive and control, precise operation and flexible movement pose synthetically. The curvature sensor, which is composed of six stain gauges, makes displacement control precise. After analyzing equilibrium of forces and moments, the numeric calculation equations are deduced. Subsequently, the approximate arithmetic making use of addible principle is researched in contrast with numeric arithmetic.

In the experiments, when the actuator operates by heating the wires w_1 and w_2 simultaneously through a current supply with the magnitude of 2 A, pulse period of 15.4 ms and variable duty ratio, the curvature is near the constant 0.8, and then increases quickly, finally reaches the maximum 28 m^{-1} as the duty ratio raises to 70 %, the maximum for single SMA wire. The actuator was shown to make a pliable motion at 55 degrees per second up to a designed maximum angle at the responding speed high enough for the purpose. The maximum angle between the tangents of two ends was 95 degree relatively. By controlling the heating of each SMA wire, the actuator could accomplish Spatial deflection flexibly.

Ankowlegement

Project Supported by National Natural Science Foundation of China (50507007) and key Foundation of Huazhong University of Science and Technology (2006).

Notations

A_f : Austenite transition finish temperature
A_s : Austenite transition start temperature
A : Surface area of the wire
c, K_s : Actuator's curvature and measurement coefficient
c_w : Specific heat of the wire
d : Distance between wires and neutral center of the rod
d_1^1 : Component in direction x_1 of the offset of the wire w_1
d_r : Duty ratio of the current
e : Elongation of the rod
E^a, I : Elastic modulus and moment of inertia of the wire
f : Distributed forces acts on the rod

F : Resultant force vector of the rod
F^a : Recovering force of the wire
f^a : Distributed force acts on the SMA wire
F_1, F_2 : Shear forces in the cross section of the rod
F_3 : Axial component force
k_1, k_2, k_3 : Two curvatures and twist of the rod
f_1, f_2, f_3 : Component forces applied on the rod from the wires
f_1^1, f_2^1, f_3^1 : Components in directions x_1, x_2 and x_3 of the wire w_1
h_w : Heat transfer coefficient
i : Electrical current
k_2 : Wire's actual curvature
k_{s1} : Curvature of the rod upon only wire w_1 being actuated
$k_1^{'}$: Recoverable curvature of the SMA wire w_1
$k_2^{'}$: Recoverable curvature of the SMA wire w_2
k_{left} : Actuator's remnants curvature
k_r : Wire's recoverable curvature
K_t : Transfer coefficient
k_{ms} : Recoverable curvature of the wire
M_s : Martensite transition start temperature
M : Resultant moment vector
m : Moment caused by f
m_1, m_2 : Component moments applied on the rod from the wires
q, L : Load density and wire length
R_r, L : Rod's radius and length
r_s : Wire's radius
$R_{ma}, R_{mb}, k_m, T_{om}$: Constants depending on whether the wire being heated or cooled
R : Wire's resistance
R_s : Standard resistance of the gauge
ΔR : Resistance change
S : The arc length along the geometric center of the rod
T_w : Wire's temperature
T : Temperature of the SMA wrie
V_s : Volume of the wire
X : Distance from calculation point to reference point
z : Neutral axis of the SMA wire
φ_{23} : Angle between the flexural plane and plane x_1x_3
ρ_w : Density of the wire
ε_1, K : Strain and the sensitive coefficient

References

Roh, S. G. and Park, K. H., 2004, "Development of Dynamically Reconfigurable Personal Robot," *IEEE International Conference on Robotics and Automation* 4(4), pp. 4023~4028.

Guan, Y. S. and Zhang, H., 2003, "Workspace of 2D Multi-fingered Manipulation," *IEEE International Conference on Intelligent Robots and Systems*, (4), pp. 3705~3710.

Bauer, S., Bauer, G. and Simona, D. et al., 2006, "Piezoelectric Polymers," *Materials Research Society Symposium Proceedings*, Vol. 889, pp. 23~30.

Hu, B., Fuchs, A. and Huseyin, S. et al., 2006, "Supramolecular Magnetorheological Polymer Gels," *Journal of Applied Polymer Science*, Vol 100, No. 3, pp. 2464~2479.

Han, L. H., Lu, T. J. and Evans, A. G., 2005, "Optimal Design of a Novel High Authority SMA Actuator," *Mechanics of Advanced Materials and Structures*, 12(3), pp. 217~227.

Singh, K., Sirohi, J. and Chopra, I., 2003, "An Improved Shape Memory Alloy Actuator for Rotor Blade Tracking," *Journal of Intelligent Material Systems and Structures*, 14(12), pp.767~786.

Yoshiyuki, N., et al., 1984, "Hitashi's Robot Hand," *Robotics Age*, 6, pp.18~20.

Mihalcz, I., Zudor, E. I., Csibi, V. and Baranyi P., 1999, "A Biomechanic Robot Hand Using SMA," *Proceedings of the Tenth World Congress on the Theory of Machines and Mechanisms*, Oulu, Finland, pp. 1835~1840.

Rush, J. A., 1997, "Memory Wire Robotic Hand," *United States Patent Number 5*, 647, 723, July 15.

Troisfontaine, N., Bidaud, P. and Morel G., 1997, "A New Inter-Phalangeal Actuator for Dexterous Mirco-Grippers," *Proceedings of the IEEE International Conference on Robotics and Automation*, Albuquerque, New Mexico, 1997, pp. 1773~1778

Burdea, 1995, "Investigation of a Shape Memory Alloy Actuator for Dexterous Force-Feedback Masters," *Advanced Robotics*, 9, pp.317~329.

Brett J De Blonk and Dimitris C Lagoudas, 1998, "Actuation of Elastomeric rods with Embedded Two-way Shape Memory Alloy Atuators," *Smart Mater. Struct*, (7), pp.771~783.

Bo, Z., Kurdila, A. J. and Lagoudas, D. C., et al., 1995, "Identification of a Class of Nonlinear Models for SMA Embedded Elastiomeric Rods," *Active Materials and Smart Structure*, 2427, pp.93~10.